Crack Extension Behavior under the Compressive Loads using the Maximum Energy Release Rate Criterion

メタデータ	言語: eng
	出版者:
	公開日: 2017-10-05
	キーワード (Ja):
	キーワード (En):
	作成者:
	メールアドレス:
	所属:
URL	http://hdl.handle.net/2297/6368

Crack Extension Behavior under the Compressive Loads using the Maximum Energy Release Rate Criterion

Chikayoshi YATOMI

Division of Global Environmental Science& Engineering, Graduate School of Natural Science & Technology, Kanazawa university, Kanazawa, Ishikawa, 920-8667, JAPAN

Yoichi SUZUKI

Technical Research Institute, GODAI Development Corp., Kanazawa, Ishikawa, 921-8051, JAPAN

Abstract - In this paper, we examine the conditions that the mode II crack extensions occur under the compressive loads. It is important to elucidate the fracture criterions under compressive loads such as the creation and the extension of the active faults or the landslide in slope ground. We first obtain the energy release rate at the onset of crack kinking under the compressive loads by the finite element method using the path independent E-integral of the complementary strain energy type. We then find, by using the maximum energy release rate criterion, that the mode II crack extension occurs by the shear stress when the minimum principal compressive stresses is relatively large. We also find that the mode II crack extensions never occur when we use the well-known maximum hoop stress criterion.

I . Introduction

The fracture surface in rock, soil, and concrete under the uniaxial compression loads or even under the multi-axial compression loads extends often straightly or curve smoothly by mode II type; that is, the crack extends as the same direction with the original crack as shown in Fig.1. In order to explain this phenomenon, most classical and important Criterion was introduced by Coulomb [1]. He suggested in connection with shear failure of rocks that the shear stress τ tending to cause failure across a plane is resisted by the cohesion of the material (or the inherent shear stress) τ_0 and the coefficient of internal friction μ times the normal stress σ across the plane. That is, that the criterion for shear failure in a plane is $\tau_0 = |\tau| - \mu \sigma$. Then he assumed that the fracture surface happens in the direction of the maximum $|\tau| - \mu \sigma$. As a result, the direction of shear fracture is always inclined at an angle to the direction of the maximum compressive stress σ_1 (See Fig.1.) as $\pi/4 - \phi/2$, where ϕ is the angle of internal friction defined by $\mu = \tan \phi$.

Although the above angle gives a good approximation in the real material, the criterion does not consider any fracture process at all. In fact, if an initial inclined crack is inserted in the material such as rock, mortar, and acrylic board, the crack surface begins to kink to the direction of maximum principal compressive stress σ_1 since the tension stresses occur near the crack tips because of the slip of the crack surface. Then the crack extends smoothly to the direction of σ_1, so that the crack becomes the wing type crack as shown in Fig.2.

Thus, from the fracture mechanics of view, it is very basic and important problem under what condition that the crack keeps extending as mode II type under the compressive loads.
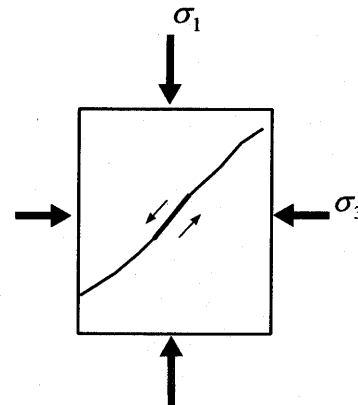

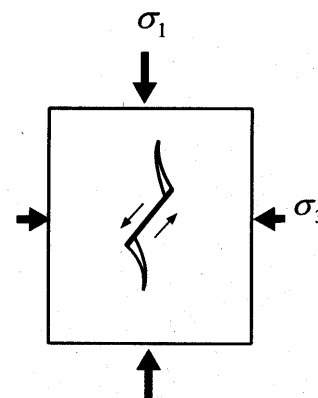Fig.1. Mode II type crack extension

Fig. 2. Wing type crack extension

Scholz and others [2] reported the experimental paper with intention of elucidating the mechanism of generating a linear long fault. Since the existence of a long shear fault is inconsistent with the existence of the wing type crack predicted by the fracture mechanics as is stated above, they regard the macroscopic long shear fault as an incorporation by the micro-cracks consisting of the wing crack.

In this paper, we examine the conditions when the mode II crack extension occurs under the biaxial compressive loads. We first obtain the energy release rate at the onset of crack kinking under the biaxial compressive loads by the finite element method using the path independent E-integral of the complementary strain energy type, in which the contact conditions with the friction along the crack surface are introduced. By using the maximum energy release rate criterion, we find that although the crack becomes the wing type crack as shown in Fig.2 when the minimum principal compressive stresses σ_3 is relatively small, the mode II crack extension occurs when the minimum principal compressive stresses are relatively large as shown in Fig.1. We finally examine the well-known maximum hoop stress criterion and find that the mode II crack extensions never occur.

II. Finite Element Analysis of Energy Release Rate at the Onset of Crack Kinking under the Compressive Loads

We obtain ERR (Energy Release Rate) at the right crack tip in 2-dimensional infinite plate under the plane stress with the compressive loads as shown in Fig.1 and Fig.2. For the analysis of the ERR of the extending crack under the compressive loads, we use the finite element method and the E-integral of the complementary strain energy type developed by our previous paper [3], in which the contact condition on the crack surface is introduced. When there exist the surface tractions such as the friction along the crack surfaces, it is proved that the path independent E-integral of the complementary strain energy type gives the higher accurate ERR at the onset of crack kinking than the original path independent E-integral [3]. The path independent E-integral of the complementary strain energy type is defined by

$$(1) \quad E(\ell) = \frac{\partial}{\partial \ell} \left[\int_{\Gamma \cap C^\pm} (\tfrac{1}{2} s \cdot u) ds \right] - \int_{\Gamma \cap C^\pm} (\frac{\partial s}{\partial \ell} \cdot u) ds ,$$

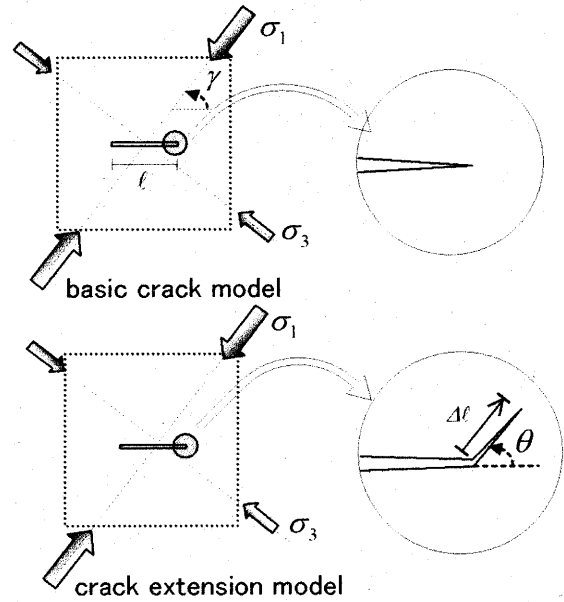where ℓ is a crack length, Γ is the boundary of an

Fig. 3. Basic crack model and crack extension model

arbitrary region in a body including a crack tip, $C^\pm$ is the upper and lower surfaces of the crack in the region. s and u are the traction and the displacement on Γ and $C^\pm$. When we obtain ERR in Eq. (1) by the finite element method, we need to analyze for the "basic crack model" with a crack length ℓ and for the "crack extension model"; that is, the crack extends the length for small length $\Delta\ell$ shown in Fig.3. The partial differentiation terms with respect to the crack length ℓ in Eq. (1) are evaluated by two points difference approximation. By using the equivalent nodal traction s_i and the nodal displacement u_i for the discretized tractions and displacements, we calculate ERR by accumulating the sum at all the nodes along an integral path, i.e., a numerical formula of Eq. (1) is as follows;

$$(2) \quad E = \sum_{i=1}^{n} \{ \frac{s_i(\ell + \Delta\ell) \cdot u_i(\ell + \Delta\ell) - s_i(\ell) \cdot u_i(\ell)}{2\Delta\ell} - \frac{s_i(\ell + \Delta\ell) - s_i(\ell)}{\Delta\ell} \cdot u_i(\ell) \},$$

where n is the total number of the nodes along an integral path, (ℓ) and $(\ell + \Delta\ell)$ mean the quantities of the basic crack model and the crack extension model, respectively.

The model used for the finite element analysis is shown in Fig. 4. The elements are 8-nodes rectangular and 6-nodes triangular isoparametric elements. We use a singular element [4][5] at the crack tip which can express the singularity of the stresses with high accuracy: We find that the singularity of the stresses cannot be expressed with high accuracy particularly for the mixed mode crack. The nodal number of the basic crack model
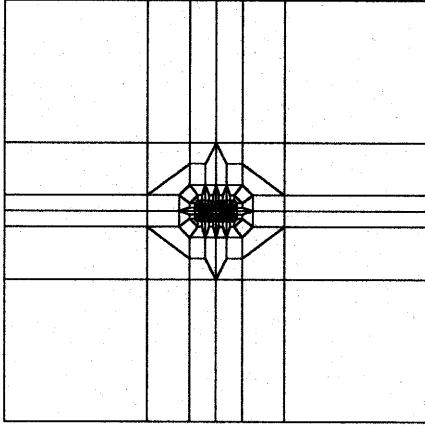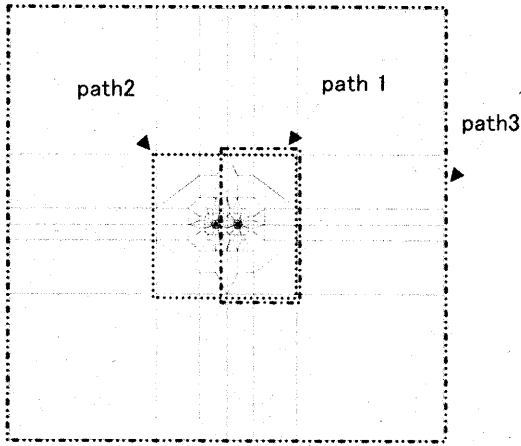
Fig. 4. Finite elements mesh

Fig. 5. Integral paths

Fig. 6. Variations of energy release rate for a frictionless kinking crack under a biaxial compression; $\gamma = 0.2\pi$; $\mu = 0.0$.

and the extension model is 920 and 922, respectively, because of releasing nodes at the crack tip for the crack extension model. The crack exists in the center of the model; an infinite plate is approximated by a square plate with the side length 80.0 cm and the crack length $\ell = 4.0$ cm. We assume that the Young's modulus E is 68.6 GPa and the Poisson ratio ν is 0.3. The ratio $\Delta\ell/\ell$ of the crack length to the extended crack length is assumed 0.0078 after doing some trial analyses by comparing with an exact solution. We consider the kinking angle θ between the angle of the load and the crack direction with nineteen directions; see Fig. 3. Here the kinking angle θ is counterclockwise positive. We consider the three kinds of integral paths which surround a right crack tip as shown in Fig.5. As a result, we found that the ERR for all analysis was almost the same value; therefore, the path independency of the E-integral in Eq. (1) holds with very high accuracy. Thus, hereafter, we use the numerical results of path3.

Here we note that the well-known J-integral is not path independent when a closed path includes more than one crack tip where the stress is singular; therefore, the values of the J-integral of path2 and path3 are the same but the value of path1 is different from the value of the other paths: Only the value of path1 gives the ERR for the case
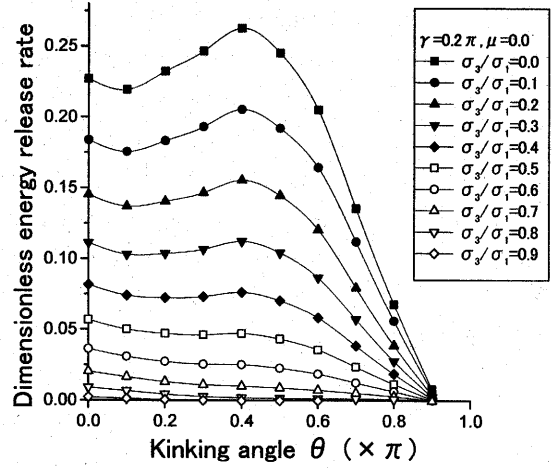
the right tip of crack extending straight. It is also very much difficult to get the ERR at the onset of the kinking crack by the J-integral.

III. Energy Release Rate at the Onset of Crack Kinking under the Biaxial Uniform Compressive Stresses

In this paper, we discuss the crack behavior by assuming the maximum ERR criterion: The crack begins to extend when the ERR reaches a critical ERR, which is a material property, and then the crack extends in the direction of the maximum ERR.

Fig. 6 depicts the dimensionless ERR at the onset of crack kinking under a biaxial uniform compressive stresses σ_1 and σ_3. We note here that σ_1 and σ_3 are the maximum and the minimum principal compressive stresses, respectively; that is, $1 > \sigma_3/ \sigma_1 \geq 0$, $\sigma_1 < \sigma_3 < 0$, and σ_2 is the intermediate principal compressive stress in the case of the plane strain and vanishes in the case of the plane stress.

The proportional loading angle $\gamma = 0.2 \pi$ ($= 36°$) as shown in Fig.3 with changing the principal stress ratio σ_3/σ_1 from 0.0 to 0.9 by 0.1 in the case of no friction on the crack surface; that is, the coefficient of friction μ $= 0$. Here the dimensionless ERR is defined as the ERR in the case of the plane stress divided by the exact solution of the ERR in the case of the plane stress with an uniaxial uniform stress in the form

(3) $$G = \frac{\sigma_1^2 \pi \ell}{2E},$$

so that the dimensionless ERR in the case of the plane stress and of the plane strain are the same.

In Fig. 6, we find that the dimensionless ERR become smaller for any kinking angle with the principal stress
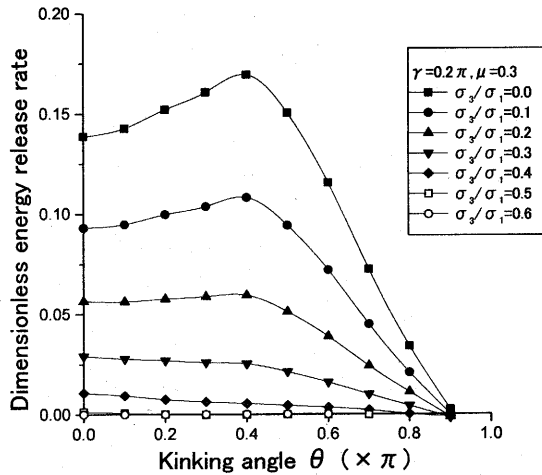
Fig. 7. Variations of energy release rate for a frictional kinking crack under the biaxial compressions; $\gamma = 0.2\pi$; $\mu = 0.3$.

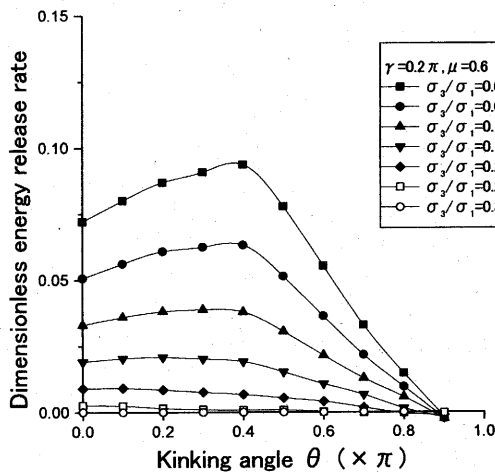Fig. 8. Variations of energy release rate for a frictional kinking crack under the biaxial compressions; $\gamma = 0.2\pi$; $\mu = 0.6$.

ratio σ_3 / σ_1 becoming bigger, that is, approaching to an isotropic stress state, $\sigma_3 = \sigma_1$: This is supposed to the shear stress near the crack tips becoming smaller with the applied stress state approaching to an isotropic stress state. We also find that for the principal stress ratio σ_3 / σ_1 from 0 to about 0.3, the maximum dimensionless ERR happens at the kinking angle $\theta \approx 0.4\pi$ ($= 72°$) , so that the crack kinks and becomes the wing crack type as shown in Fig.2: However, for the principal stress ratio σ_3 / σ_1 from 0.4 to about 0.9 , the maximum dimensionless ERR happens at the kinking angle $\theta = 0°$, so that the crack extends as the same direction with the original crack as shown in Fig.1

Fig. 7 and Fig. 8 depict the dimensionless ERR at the onset of crack kinking under a biaxial uniform compressive stresses σ_1 and σ_3 for the same proportional loading angle $\gamma = 0.2\pi$ ($=36°$) as before when there exists
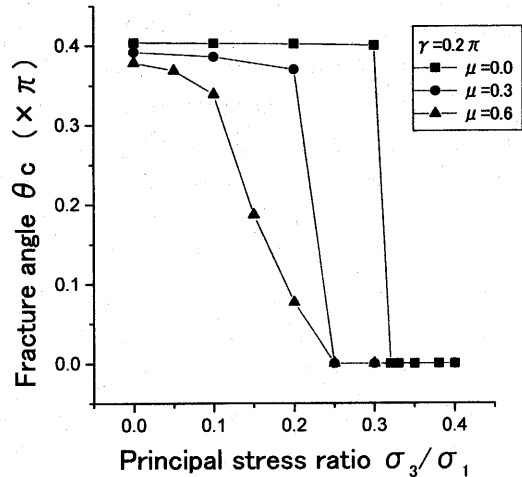

Fig. 9. Relations between the principal stress rate and the kinking angle which maximizes the energy release rate; $\gamma = 0.2\pi$; $\mu = 0.0, 0.3, 0.6$.

the friction along the crack surface. In Fig.7, the principal stress ratio σ_3 / σ_1 change from 0.0 to 0.9 by 0.1 with the coefficient of friction $\mu = 0.3$: Here we note that when the principal stress ratio σ_3 / σ_1 becomes bigger than 0.6, we omit the lines in the figure since the dimensionless ERR vanishes for all kinking angle.

In Fig.8, the principal stress ratio σ_3 / σ_1 changes from 0.0 to 0.3 by 0.05 with the coefficient of friction $\mu = 0.6$. By the same reason as above , when the principal stress ratio σ_3 / σ_1 becomes bigger than 0.3 , we omit the lines in the figure .

Fig. 9 depicts the relation between the principal stress ratio σ_3 / σ_1 and the fracture angle θ_c, which is the maximum ERR at the onset of crack kinking under a biaxial uniform compressive stresses σ_1 and σ_3 for the proportional loading angle $\gamma = 0.2\pi$ ($= 36°$).

In Fig.9 , solid lines with ■ , ●, and ▲ show the fracture angel in the case of $\mu = 0.0$, $\mu = 0.3$, and $\mu = 0.6$, respectively.

In the case of $\mu = 0.0$, for the principal stress ratio σ_3 / σ_1 bigger than 0.3, the maximum dimensionless ERR happens at the kinking angle $\theta = 0°$, so that the crack extends as the same direction with the original crack as shown in Fig.1. In the cases of $\mu = 0.3$ and $\mu = 0.6$, for the principal stress ratio σ_3 / σ_1 bigger than about 0.25, the maximum dimensionless ERR happens at the kinking angle $\theta = 0°$. In the case of $\mu = 0.0$, fracture angle decreases at the principal stress ratio σ_3 / σ_1 about 0.3 suddenly. We may recognize this by Fig.6 in which the curve between the kinking angle 0.0π and 0.4π is convex downward, the kinking angle of the maximum of the fracture angle jumps from 0.4π to 0.0π at the principal stress ratio σ_3 / σ_1 about 0.3.

Finally, instead of the maximum ERR criterion, we examine the maximum hoop stress criterion in which we use the exact asymptotic expansion terms of the hoop stress in the vicinity of the crack tip: Here we obtain the first singularity term and the constant term, which is called the T stress, for a biaxial uniform compressive stress when there exists the friction along the crack surface. We then find that the maximum hoop (tension) stress happens at the kinking angle about $\theta \approx 0.4\,\pi$ (=72°) for any principal stress ratio σ_3 / σ_1, so that the crack always kinks and becomes the wing type crack as shown in Fig.2. no matter how large the principal stress ratio σ_3 / σ_1 (< 1)becomes . In other words, the maximum hoop stress criterion never extends a crack as the same direction with the original crack as shown in Fig.1.

The maximum hoop stress criterion use the stress at the crack model before the kinking, so that however large the minimum principal compressive stresses σ_3 becomes, the hoop tension stress is created and becomes its maximum at around $\theta \approx 0.4\,\pi$ (=72°) because of the slip of the crack surface counterclockwise as in Fig.2. On the other hand, in the maximum ERR criterion, we consider the state after the crack kinking. Then the minimum principal compressive stresses σ_3 suppresses the opening the kinked part of the crack with the direction of about $\theta \approx 0.4\,\pi$ (=72°) and make the ERR of the crack in its direction smaller. When the minimum principal compressive stress σ_3 becomes larger, the ERR finally takes its maximum in the direction with the original crack. The friction makes the above effect bigger.

Reference

[1] J. C. Jaeger, N. G. W. Cook, *Fundamentals of Rock Mechanics*, Methune & Co Ltd, London,1969.

[2] S. J. D. Cox, C. H. Scholz, "On the formation and growth of faults: an experimental study, " *Journal of Structural Geology* Vol. 10, pp. 413-430, 1988.

[3] C. Yatomi, Y. Suzuki, "Finite element analysis of the energy release rate by using the E-integral under compressive loads, " JSCE No.612, I-46, pp.251-263, 1999 (in Japanese).

[4] R. S. Barsoum, " On the use of isoparametric finite elements in linear fracture mechanics," *International Journal for Numerical Methods in Engineering* Vol. 10, pp. 25-37, 1976.

[5] R. S. Barsoum, "Triangular quarter-point elements as elastic and perfectly-plastic crack tip elements," *International Journal for Numerical Methods in Engineering* Vol. 11, pp. 85-98, 1977.